feedback was provided using an invasive approach. During object recognition of different properties, multiple sources of sensory feedback are needed [21], [22]. Noninvasive multi-source feedback approaches have been evaluated in previous studies [23]–[25]. Some have shown improvement in prosthetic functionality [25] and distinguishability of haptic cues [24], while others have reported degraded control when compared to single feedback sources [23]. Nonetheless, most of these approaches elicited solely haptic feedback. As a result, it remains unclear how concurrent haptic and tactile-proprioceptive feedback sources are used at different myoelectric control strategies.

Accordingly, the purpose of the current study was to evaluate object recognition using a specific non-invasive multimodal sensory stimulation when participants myoelectrically controlled a prosthetic hand. Specifically, we examined how different types of somatosensory (haptic and tactile-proprioceptive) information were integrated for different types of controllers (position- vs. velocity-based control) for object recognition (size and stiffness). We hypothesized that position control would result in greater recognition accuracies, because the EMG-position mapping is more intuitive and muscle activation level could provide additional information about the joint angle. Haptic feedback was elicited via transcutaneous stimulation of the peripheral nerves, using an electrode grid placed along the upper arm targeting the median and ulnar nerves [7]–[9], [26]. Spatially distinct sensations could be evoked by recruiting distinct sensory axons [27]. In contrast, nerve stimulation is less likely to elicit tactile-proprioceptive sensation, which is commonly provided using sensory substitution [28]–[31]. We elicited tactile-proprioceptive feedback describing the prosthetic's joint kinematics using a vibrotactor array placed on the upper arm. The prosthetic hand was myoelectrically controlled using either position- or velocity-based control. During prosthetic control, fingertip forces were transformed to amplitudes of nerve stimulation, while the joint angles of the index finger were translated to distinct vibratory parameters (location and intensity). This unique design allowed us to evaluate the integrative role of artificial tactile-proprioceptive feedback and somatotopic haptic feedback for the recognition of multiple object properties concurrently, when different myoelectric controllers were employed. Prior work has evaluated the recognition of a single object property using force feedback approaches [32], [33]; however, artificial feedback of multiple modalities (either invasive or non-invasive) has yet to be assessed to the same extent, especially when discerning their interaction with various control strategies. Additionally, concurrent recognition of multiple object properties has not been tested non-invasively with myoelectric control. The current study can help us understand the impact of concurrent haptic and tactile-proprioceptive feedback on closed-loop control of prosthetic hands during object recognition. Our novel haptic feedback approach also elicits somatotopic percepts that are deemed more intuitive compared to typical sensory substitutional perceptions [34], thereby potentially reducing the cognitive load. The non-invasive feedback strategies can also be refined, and applied on a greater number of individuals with various clinical populations.

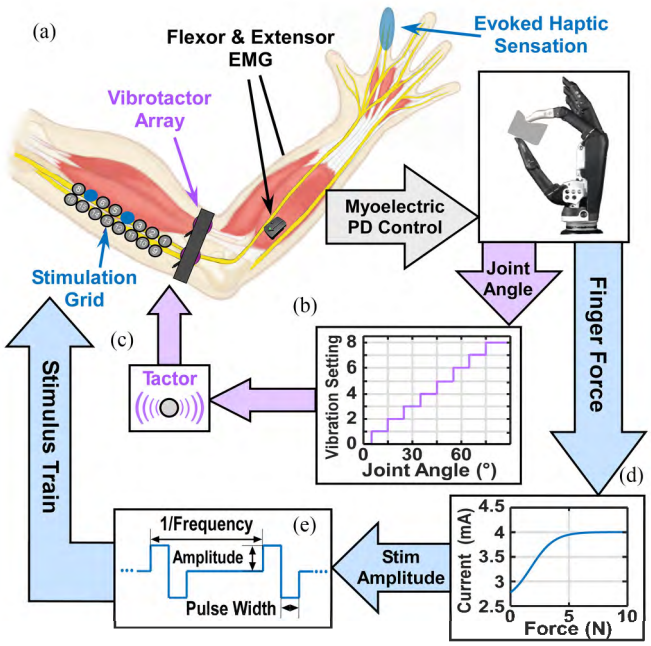

Fig. 1. Diagram illustrating the location of the vibrotactors, 2x8 electrode grid, and EMG channels (a) along with the sensory feedback approach. The joint angle and fingertip force from the sensorized prosthetic hand was used to elicit tactile-proprioceptive (b, c) and haptic feedback (d, e), respectively. Joint angle was converted to a tactor setting (b) eliciting vibratory feedback (c). Fingertip force was converted to a desired current amplitude using a user-specific sigmoid function (d) to generate the stimulation train (e).

II. Methods

A. Participants

Nine neurologically intact participants (6 Male, 3 Female, 23–30 years of age) and one amputee (Female, 6 years after amputation) were recruited for this study. Informed consent was received from each participant via protocols approved by the Institutional Review Board of the University of North Carolina at Chapel Hill (Approval #: 16-1852). All participants were naïve about the experimental protocol.

B. Experimental Setup

Each participant was seated in front of a table with their right arm placed comfortably atop of it. The medial and lateral sides of the upper arm and forearm were then cleaned using alcohol pads. Using the line connecting the medial epicondyle of the humerus to the center of the axilla as a reference, a 2x8 electrode grid was positioned across the medial side of each participant's upper arm (Fig. 1a). The median and ulnar nerves are superficial to the skin near this location, allowing for electrical stimulation to elicit haptic feedback along the hand. By stimulating distinct pairs (i.e., bipolar stimulation), unique electric field activated unique sensory axons that innervate discrete hand regions. Following grid placement, a plastic vice applied mild pressure ensuring stable electrode-skin contact.

A custom MATLAB interface (v2017b, MathWorks Inc) communicated with a switch matrix (Agilent Technologies) and an electrical stimulator (STG4008, Multichannel System) to

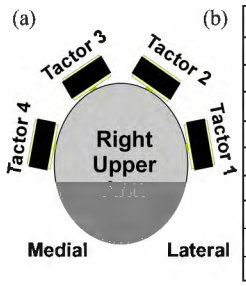

Tactor Setting	Angle Range (°)	Tactor #	Tactor Strength
OFF	< 5	None	Off
1	5 - 14.99	1	Low
2	15 - 24.99	1	High
3	25 - 34.99	2	Low
4	35 - 44.99	2	High
5	45 - 54.99	3	Low
6	55 - 64.99	3	High
7	65 - 74.99	4	Low
8	75 - 85	4	High

Fig. 2. Diagram illustrating the placement of the vibrotactor array in relation to the right upper arm of the participant (a). Each combination of tactor and stimulation level corresponds to a given prosthetic joint angle range (b).

delivery stimulation trains to designated electrode pairs. The matrix linked the cathode and anode of the stimulator to one of sixteen Ag/AgCl gel-based electrodes. Using a fixed pulse width (200 μs) and frequency (150 Hz) [26], [27], the stimulator delivered biphasic, charge-balanced, square waves with amplitudes modulated by the fingertip force from the I-limb Ultra prosthetic hand (Robo-limb, Ossur) (Fig. 1e).

A band of vibrotactors was wrapped around the upper arm just proximal to the participant's elbow (Fig. 1a). The band consisted of 4 tactors (3.05 cm diameter C-2 Tactor, ATAC) each spaced approximately 6 cm apart (center-to-center). Tactors 1 and 2 were positioned along the laterial side of the upper arm, while tactors 3 and 4 were placed on the medial side (Fig. 2a). The band was then gently tightened to ensure sufficient skin contact. Participants were asked and reminded to report any discomfort throughout the experiment.

Vibration timing, amplitude, and frequency for each tactor was specified through a controller (ATAC) programmed by the MATLAB interface. During the study, the frequency was fixed at 200 Hz, because human skin was most responsive to values between 200-250 Hz [14]. Four tactors and two stimulation levels were combined to represent eight discrete finger positions along the prosthetic index finger's range of motion (Fig. 2b). Eight finger positions, 10 degrees apart, were selected to match the natural proprioceptive acuity of the hand in healthy individuals [35]. A low and high stimulation level was executed using RMS amplitudes of 151 and 300 mA, respectively. These parameters produced sensory feedback without eliciting tendon illusion [36]. The use of multiple tactors minimized the potential for irritation and desensitization of the skin [37] and increased user intuitiveness. To further minimize desensitization, vibration transitions to an idle state when the robot's joint angle was held constant for longer than 2 seconds. In this state, one second of stimulus was delivered to provide users with feedback once every 3 seconds. The system returns to its normal state once movement was resumed.

Electrical and vibratory stimulation were modulated concurrently in real-time based on the force and joint angle recordings from the prosthetic hand, respectively. Specifically, current amplitudes were defined by transforming the recorded forces using a participant-specific sigmoid function (Fig. 1d). The function was constructed using a minimum of 0.10 N and maximum of 5 N force, an allowable stimulation range, and a steepness value of 1 [8], [9]. The minimum and maximum forces were selected via preliminary test. The minimum value ensured stimulus was not continuously delivered if force sensor drift occurred. The maximum value was set to a value slightly below the average peak force exerted when grasping the softest objects, which ensured that stiffness was identified based on the rate of change of the stimulus strength rather than the peak intensity. For each participant, the stimulation range was bound using the sensory threshold and just below the motor threshold for the selected electrode pair (Table I). The sensory threshold was identified as the stimulation amplitude that initially evoked haptic sensation on the fingers of the participants. The motor threshold was identified as the stimulation amplitude that evoked visible motion of the finger. For each threshold identification process, the amplitude was set to a random value and was slowly increased using a step of 0.1 mA until the given threshold was identified. The upper limit amplitude was set to one to two steps below the motor threshold to minimize the potential for muscle contractions. This process was repeated three times for each threshold, and the three outcomes were then averaged to find the stimulation range. The flattening of the sigmoid curve ensured participant safety and further reduced the likelihood of inducing muscle activations.

TABLE I
STIMULATION PARAMETERS FOR INDIVIDUAL PARTICIPANTS

Participant #	Sensation Region: I: Index, M: Middle, R: Ring, T: Thumb	Electrode Pair (Cathode – Anode)	Sensory Threshold (mA)	Just Below Motor Threshold (mA)
Intact1	I & M	4-6	1.5	2.0
Intact2	I	2-5	3.9	6.0
Intact3	I & M	3-6	3.2	3.7
Intact4	I & T	11-13	1.3	5
Intact5	I, M & R	3-5	2.8	3.8
Intact6	I & R	11-13	2.8	3.6
Intact7	I	5-7	3.5	4.4
Intact8	I & M	2-4	2.7	3.6
Intact9	I	4-7	3.1	3.9
Amputee1	I, M, & T	2-5	1.6	2.5

The joint angle relating to the metacarpophalangeal (MCP) joint of the prosthetic's index finger was used to modulate the tactor vibration to provide tactile-proprioceptive feedback to the user. The desired setting was determined using discrete mapping of the joint angle to one of the eight tactor settings (Fig. 1b and 2b). The encoding resolution was 10 degrees.

C. Myoelectric Control

The prosthetic hand was placed on a stand in front of the experimenter to ensure that incidental feedback, such as the vibration of the prosthetic, would not be provided to the participants. Visual feedback was blocked by placing the hand outside of the participant's line of sight. Noise-canceling headphones were also used to block the audio cues from the devices. The prosthetic's index finger was myoelectrically controlled by the participant. Two electromyogram (EMG) electrodes (Delsys

Trigno) were placed on the anterior and posterior sides of the participant's forearm (Fig. 1a) to record the activities of extensor digitorum communis and flexor digitorum superficialis of the index finger, respectively. Using a 200-ms window with 100-ms overlap, the activation level was extracted from the rectified and filtered EMG signals after normalization by the maximum voluntary contraction (MVC) for each channel. The joint angle or velocity was linearly mapped in real-time based on the relative muscle activation level with the maximum values corresponding to 50% MVC to minimize potential muscle fatigue. By comparing the relative extensor and flexor activation levels, the direction and speed in which the prosthesis articulates was determined using position- or velocity-based control schemes. Position-based control mapped the relative level of activation to a given finger position, e.g., a relatively higher flexor activation than extensor resulted in a greater joint flexion angle. The joint angle of the prosthesis can move from 0–85° of flexion with a minimal controllable angle of ~1.25°, as a result 2-degrees of error tolerance was set for the reference angle. For velocity-based control, the relative level of flexor and extensor activation was mapped to the joint speed. For this prosthetic hand, the minimum and maximum angular velocity was approximately 25° and 80° per second, respectively. A custom-made proportional derivative (PD) controller was implemented using MATLAB to control the position or velocity of the finger. The controller updated the reference position or velocity at 10 Hz, and the control command to the motor was updated at 40 Hz.

D. Experimental Procedure

Pre-experimental preparations were performed. First, each vibratory setting was stimulated to ensure the stimulus did not cause any pain or discomfort. Next, the electrode grid was searched to find an electrode pair and stimulation range that elicited sensation along the individual's index finger (Table I). Each participant then practiced controlling the prosthetic hand using each control scheme for 1–2 minutes. Participants were then introduced to each of the 8 vibratory settings. During this period, the experimenter informed the participant of which joint angle the stimulus represented. The vibrator settings were elicited in order from 10 to 80 degrees and back to 10 degrees.

The main experiment evaluated the recognition performance of objects of varying size and stiffness with haptic and tactile-proprioceptive feedback simultaneously. Based on the prosthetic fingertip force, stimulation intensity was altered during object grasping. Object recognition was performed using four cubes: two sizes (4 cm and 6 cm) and two stiffness levels (1.7 N/mm and 2.9 N/mm). Object size was encoded as the sensed joint angle (tactor location and vibration intensity) when the prosthetic finger contacted the cube, while the rate of change of the electrical stimulation intensity was used to discriminate object stiffness.

We tested position and velocity control in two blocks. These two control schemes were executed in a random order across participants. Prior to each control scheme, participants explored the two types of sensory percepts as they grasped various objects using the prosthesis. After 2–3 minutes of exploration, visual and auditory information was blocked prior to a short training period (10–15 trials) with feedback of performance provided. The experimenter placed the object in a random order between the prosthetic's index finger and thumb. Participants were instructed to flex the prosthetic's index finger to grasp the object, and report the perceived size and stiffness. After training, participants completed 3 trials per object totaling 12 trials per block. The amputee participant performed 4 trials per object for a total of 16 trials per block. During these trials, participants were not given feedback about their responses. Example force and joint angle traces produced during a given object grasp are shown in Fig. 3. *Supplementary videos* demonstrate the closed-loop control of the prosthesis during object recognition.

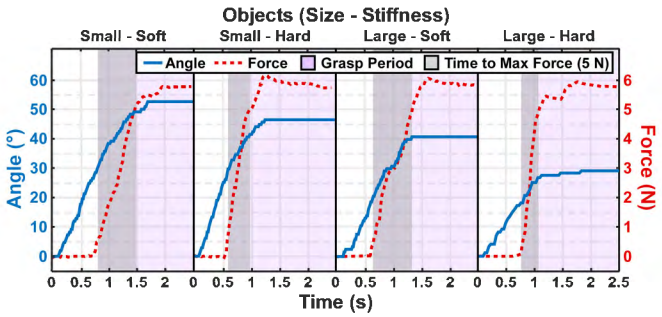

Fig. 3. Example force (red) and joint angle (blue) traces when grasping the four objects of varying size and stiffness. The gray region indicates the time needed to reach the maximum force of the sigmoid function.

E. Data Analysis

To evaluate the recognition accuracy, confusion matrices were constructed to compare the ground truth with the recognized object. The average and standard error of the evaluation metrics were calculated across participants.

F. Statistical Analysis

One sample Wilcoxon signed rank test were conducted for each testing condition to evaluate if recognition accuracies were significantly greater than chance values. The chance of correctly identifying both the size and stiffness of the object was 0.25. Additionally, a chance value of 0.5 was utilized to assess the recognition of object size or stiffness individually. Lastly, paired Wilcoxon signed rank tests were performed to assess the effect of control schemes and feedback conditions. To control the risk of type I error when performing multiple statistical tests, a Bonferroni-based correction was applied to the p-value of 0.05 [38].

III. Results

We evaluated the recognition performance of object size and stiffness using the position or velocity control scheme. The objects were labeled with 'S-S' denoting a small-soft object, 'S-H' denoting a small-hard object, 'L-S' denoting a large-soft object, and 'L-H' denoting a large-hard object. The confusion matrices (Fig. 4) evaluate the perceived object size and stiffness to the ground truth. The results showed that most objects

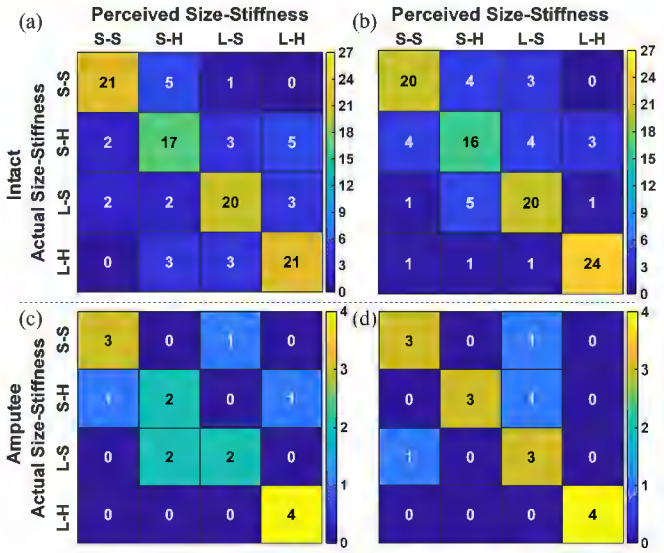

Fig. 4. Confusion matrices comparing the actual and perceived object size and stiffness when grasping various objects using position (a) and velocity (b) based control across all intact participants. Position (c) and velocity (d) control conditions of the amputee. 'S-S': small-soft, 'S-H': small-hard, 'L-S': large-soft, and 'L-H': large-hard. .

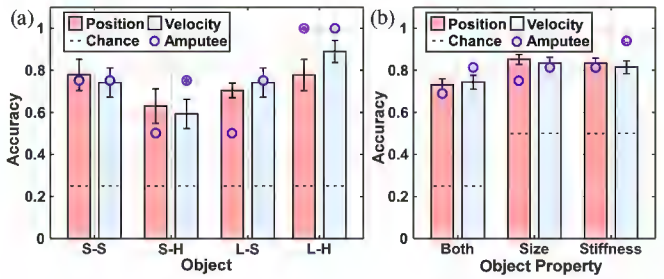

Fig. 5. The identification accuracy of individual objects (a) and object property (b) averaged across all intact participants (bars). The filled circles represent the accuracy of the amputee participant. 'S-S': small-soft, 'S-H': small-hard, 'L-S': large-soft, and 'L-H': large-hard. Error bars denote standard error.

were correctly identified when using both position and velocity control, with an accuracy of 73.1% ± 2.5% and 74.1% ± 3.1% for intact participants, respectively. The corresponding accuracy levels were 68.8% and 81.3% for the amputee, which were similar to the intact participants. Most of the errors were observed when recognizing the L-S and S-H objects. All recognition accuracies were found to be significantly greater than chance ($p<0.05$, power > 0.8) with no significant difference across control conditions ($p > 0.05$).

The recognition accuracy varied across the four objects (Fig. 5a). When utilizing velocity control, the L-H object was identified correctly most often by intact participants, resulting in an accuracy of 89.0% ± 5.2%; however, the S-S object showed the highest accuracy (77.9% ± 7.4%) when utilizing position control. Similarly, the amputee showed a 100% accuracy when identifying the L-H object using both control schemes. Across both control schemes, the lowest recognition accuracy was reported when grasping the S-H object for intact participants. The S-H object was correctly identified during 63% of position-control trials and during 59% of velocity-control trials. The amputee also showed the lowest accuracy (50%) when recognizing the S-H and L-S objects using position-control, and a higher accuracy (75%) was observed on these two objects when using velocity-control. Nevertheless, all four objects resulted in recognition accuracies significantly greater than chance value ($p < 0.05$, power > 0.8). When comparing across control schemes, no significant differences were observed, except for the L-H object. Velocity-control resulted in a statistically greater recognition accuracy ($p < 0.05$), compared to position-control.

When evaluating each individual property, object size and stiffness could each be identified separately (Fig. 5b). During position and velocity control, object size recognition resulted in accuracies of 85.1% ± 2.2% and 83.3% ± 2.6% for intact participants, respectively. The corresponding accuracy levels were 75% and 81.3% for the amputee. Object stiffness was correctly identified when using both position and velocity control, with an accuracy of 83.3% ± 2.3% and 81.4% ± 2.9% for intact participants, and 81.3% and 93.8% for the amputee. Additionally, for both control schemes, the recognition accuracies of individual object property were significantly greater than chance value ($p<0.05$, power > 0.8). For each property, no significant difference was observed between control conditions ($p > 0.05$).

IV. Discussion

The current study sought to determine how non-invasive somatosensory feedback affects object recognition with distinct myoelectric control schemes. Our findings show that concurrently evoked haptic and tactile-proprioceptive feedback allowed for accurate object property recognition. The outcomes can facilitate our understanding of the sensorimotor integration process during human-robot interactions, which can potentially promote fine control of prosthetic devices.

Our results showed that participants effectively performed object size and stiffness recognition via concurrent haptic and tactile-proprioceptive feedback in either position- or velocity-control schemes with similar performance. It is possible that a simple open and closing task may have caused the similarity in response accuracy, especially in naïve participants. A task with higher complexity or involving object manipulation could potentially distinguish the two types of controllers. In the future, we plan to perform more in-depth evaluations of the stimulation approach in more ecological settings, where the task includes reaching, grasping, manipulation, and releasing. Although the amputee participant demonstrated identification accuracy levels largely similar to the intact participants, the accuracy levels varied based on the controller, with greater accuracies observed in velocity-control. The amputee participant described that position-control provided greater controllability of the hand; however, the added control effort of maintaining greater muscle activation levels could have affected the recognition accuracies. These outcomes represent the participants (both intact and amputee) that had no prior experience with the stimulation approaches.

Our results also showed that all four objects could be recognized with accuracies significantly greater than chance; however,

the lowest accuracy (<60%) arose when attempting to recognize the small-hard object. The joint angle encoding resolution was 10 degrees in our case. As shown in the example traces in Fig. 3c, the difference in the joint angles at object contact between the small-hard and large soft was <10 degrees. As a result, the object size recognition is likely affected by the low encoding resolution in joint angle. In addition, some participants had lower stimulation range (motor-sensory threshold). Prior work has shown that lower ranges can result in reduced accuracy when discerning stiffness [7]. A lower range reduces the number of perceived stimulation (sensation) levels and in turn the resolution of the elicited haptic information. Altering the stimulation waveform through reductions in pulse width and the addition of an interphasic delay can potentially improve the resolution of haptic encoding. Alternatively, the mapping of the EMG to a given position/velocity may affect the accuracy. Restricting the maximum speed can allow for more time to perceive the change in haptic sensation intensity and identify the tactor setting when the finger contacts an object. As a result, stiffness and size recognition may be improved, allowing for the recognition of a greater range of sizes and stiffness levels [7].

Lastly, a single feedback has shown differing levels of success when discerning stiffness. Some studies reported accuracies similar to those reported in the current study [5], [7], while others reported lower accuracy values [18], [33]. The reduction in accuracy may be due to the greater number of object stiffness levels assessed and/or feedback method used. Prior work reported improved accuracy and response time when identifying a stimuli's position and intensity if the feedback was somatotopic [34]. The greater success rates reported here may also be attributed to the added insight provided by a specific multimodal feedback approach. However, multiple feedback sources can also require more workload, given that both are not as natural as the biological feedback. Combining multiple feedback sources can cause a synergetic effect that alters perception of a particular stimulation. In addition, excessive information can lead to sensory overload affecting perceptibility of a given feedback source. Prior work has supported the use of multimodal systems for improving the perceptual accuracy of complex feedback information, such as haptic and proprioceptive cues [39], [40]. However, one study suggested that cognitive load likely affects sensory acuity [24]. Prior work has shown that somatotopic feedback was more robust to dual tasks compared to substitutional strategies [41]. The results suggest that our somatotopic feedback approach may limit the cognitive load, which could decrease the potential loss of sensory acuity. Nevertheless, future work is needed to evaluate the cognitive load during multimodal feedback in order to optimize these feedback modalities.

Prior studies have shown that recognition of object size and stiffness can be performed using invasive techniques [20], [29]. Our current non-invasive approach resulted in accuracies that were slightly lower than those reported in prior work. Variations in the accuracies were likely affected by differences in training/user experience, experimental protocol, prosthetic controller, and object characteristics. In our study, the participants received minimum training with the elicited sensory feedback. The amount of prior training and experience with a prosthesis or sensory feedback strategy can affect an individual's perception of the elicited sensations. Regarding the experimental protocol, earlier work [20] evaluated the recognition of object size and stiffness separately, potentially reducing the complexity of size and stiffness interactions. Regarding the prosthetic controller, our study evaluated the difference in recognition accuracy when utilizing continuous position- and velocity-control schemes. A previous work [29] utilized a pattern classification of three states (hand open, hand close, and rest) using a fixed articulation speed. In this case, a fixed speed reduces the variability in exerted forces and finger movement, improving the consistency across trials. Lastly, the differences in object size and stiffness in different studies may affect the produced force and joint angle, including the contact timing and rate of change of the evoked sensory feedback. Overall, our findings suggest that object size and stiffness recognition can be performed using non-invasive sensory stimulation, which allows for routine testing across a larger population and eliminates the need for surgical procedures.

Haptic feedback was elicited by stimulating the peripheral nerves, evoking feedback based on the force exerted by the prosthesis. Unlike fingertip haptic feedback, tactile-proprioceptive feedback is often conveyed using sensory substitutional techniques. In the current study, 4 tactors were placed along the distal region of the upper arm. This setup was selected to distribute the vibratory stimulus across multiple locations of the skin surface. This design limited the possibility of sensory adaptation or habituation due to continued activation at a single location, if a single tactor is used. Sensory adaptation can affect user's perceptual accuracy, which could impact the closed-loop control of the device [42]. Although the tactor controller can activate multiple tactors concurrently, a prolonged activation of a previous active tactor could lead to sensory habituation. A higher number of stimulation levels can also provide greater number of encoded angles. However, during muscle contraction or limb movement, the contact between the skin and the tactor could change, which could bias the perceived stimulation levels. Therefore, we used only two stimulation levels. In addition, 8 settings were selected to mimic the proprioceptive acuity of the finger with the change in vibration intensity and location mirroring the finger's motion. If greater angle resolution were needed, stimulation levels or tactors could be added to improve system performance [43].

The non-invasive nature of our technique could be employed with other prosthetic devices as well. Other devices could be used in the place of the current prosthesis if force and joint angle information can be recorded. One study has shown that the SoftHand Pro can lead to greater functional outcomes compared with typical devices used by recruited amputees [44]. Pairing this feedback strategy with the SoftHand Pro could close the loop, further improving system functionality. The non-invasive nature also allows for use in alternative settings. For example, this approach can potentially be implemented for other clinical populations, such as individuals with sensory deficits, post-stroke survivors, or for the utility of teleoperated devices. Sensory deficiencies can potentially be restored with enhanced sensory feedback, and individuals with sensory impairments can perceive the evoked haptic and tactile-proprioceptive feedback

to allow for improved control of their limb. In stroke populations, significant correlation between upper limb motor and somatosensory impairments has been reported [45]. Underlying somatosensory impairments, including reduced haptic and proprioceptive sensations, can negatively affect the execution of motor tasks [46]. In addition, functional imaging suggest that motor training leads to heightened somatosensory cortex activation [47]. Thus, synchronized somatosensory and motor training can potentially strengthen the activation of both cortical regions leading to supplemental benefits during rehabilitation. Like prosthetic devices, teleoperated devices have advanced in recent years. Accurate device operation can be challenging for the user when the device interacts with objects of varying properties, such as stiffness, size, and weight [48]. In general, a teleoperation system should be intuitive enough to allow users to easily control the end-effector, in order to efficiently and safely perform a given task [49]. Sensory feedback provides insight into the interaction between the user and the device in a remote setting, which can ensure successful task performance [50]. The elicited multimodal feedback could enable dexterous control by pairing our stimulation approach with a teleoperated device. Nonetheless, future investigations are needed to evaluation the possible outcomes from these alternative applications.

The current study has several limitations. First, evaluations were performed with a limited number of trials and participants spanning both intact and amputee populations. In terms of amputee recruitment, a prior study identified that the haptic percepts elicited via transcutaneous electrical nerve stimulation is similar between individuals with and without arm amputations [27]. In addition, similar recognition accuracies were observed between the amputee and the intact participants in the current study. As a result, outcomes seen in intact participants may characterize those expected in amputees. Unlike the plastic behavior of the motor cortex representation, several years following an amputation, the phantom hand's somatosensory cortex representation remains s [51]. In addition, several studies, comparing the spatial acuity of an amputee's residual and intact limbs, suggest that the touch and two-point discrimination thresholds were better on the residual limb [30], [52]. The improvements are potentially due to either the reorganization of the central sensory mapping [53] or the attentional resources that can prioritize use after amputation [54]. Nevertheless, further investigations involving a larger number of arm amputees are necessary to examine whether the findings remain consistent in this population. A small number of trials were tested in each condition to limit the duration of the experiment. In the future, a greater number of trials can be performed to ensure observations remain consistent over multiple sessions. Second, the study utilized an array of tactors to represent the kinematics of a single finger. Daily tasks typically require multiple fingers to perform a variety of grasp patterns. Encoding of multi-finger proprioception can be employed by varying the vibration frequency or through temporally varied stimulation pulses. During myoelectric control of the prosthesis joint, EMG variations and inconsistency of object placement in the hand could lead to variations of vibrotactile feedback for the same object. It is unlikely that the participants used a fixed vibration setting to indicate a specific object. However, it would be meaningful to evaluate the recognition of a range of objects not used during the initial training. Last, the control schemes applied were relatively simple with proportional control based on the EMG amplitude of two channels. The simplification of the control strategy allowed for a direct evaluation of prosthetic control and object recognition during position- and velocity-control with and without feedback. Nevertheless, it is crucial to evaluate whether these findings can hold with more complex control strategies, such as musculoskeletal model-based control or motor unit-based control approaches [55]–[58].

V. Conclusion

Overall, our study demonstrated that non-invasively evoked haptic and tactile-proprioceptive feedback could enable object recognition tasks using continuous position- and velocity-control schemes. Our findings highlight the integrative role of multiple feedback modalities during object recognition. The outcomes suggest that this sensation encoding strategy can potentially improve the control of sensorized prosthesis or remotely controlled devices. The elicited sensory information could improve user confidence and experience. The sensory stimulation approach can also offer an evaluation platform to understand the sensorimotor integration processes during bidirectional human-machine interactions.

References

[1] K. Li, Y. Fang, Y. Zhou, and H. Liu, "Non-invasive stimulation-based tactile sensation for upper-extremity prosthesis: A review," *IEEE Sens. J.*, vol. 17, no. 9, pp. 2625–2635, May 2017.

[2] B. T. Nghiem *et al.*, "Providing a sense of touch to prosthetic hands," *Plast. Reconstr. Surg.*, vol. 135, no. 6, pp. 1652–1663, Jun. 2015.

[3] J. A. George, M. R. Brinton, P. C. Colgan, G. K. Colvin, S. J. Bensmaia, and G. A. Clark, "Intensity discriminability of electrocutaneous and intraneural stimulation pulse frequency in intact individuals and amputees," *Annu. Int. Conf. IEEE. Eng. Med. Biol. Soc.*, Jul. 2020, pp. 3893–3896, Jul. 2020.

[4] J. S. Schofield, K. R. Evans, J. P. Carey, and J. S. Hebert, "Applications of sensory feedback in motorized upper extremity prosthesis: A review," *Expert Rev. Med. Devices*, vol. 11, no. 5, pp. 499–511, 2014.

[5] S. Raspopovic *et al.*, "Restoring natural sensory feedback in real-time bidirectional hand prostheses," *Sci. Transl. Med.*, vol. 6, no. 222, Art. no. 222ra19, Feb. 2014.

[6] K. Horch, S. Meek, T. G. Taylor, and D. T. Hutchinson, "Object discrimination with an artificial hand using electrical stimulation of peripheral tactile and proprioceptive pathways with intrafascicular electrodes," *IEEE Trans. Neural Syst. Rehabil. Eng.*, vol. 19, no. 5, pp. 483–489, Oct. 2011.

[7] L. Vargas, H. Huang, Y. Zhu, and X. Hu, "Stiffness perception using transcutaneous electrical stimulation during active and passive prosthetic control," *Annu Int Conf IEEE Eng Med Biol Soc*, Jul., 2020, pp. 3909–3912.

[8] L. Vargas, H. Huang, Y. Zhu, and X. Hu, "Object shape and surface topology recognition using tactile feedback evoked through transcutaneous nerve stimulation," *IEEE Trans. Haptics*, vol. 13, no. 1, pp. 152–158, Jan. 2020.

[9] L. Vargas, H. Shin, H. H. Huang, Y. Zhu, and X. Hu, "Object stiffness recognition using haptic feedback delivered through transcutaneous proximal nerve stimulation," *J. Neural Eng.*, vol. 17, no. 1, Dec. 2019, Art. no. 016002.

[10] V.E. Abraira and D. D. Ginty, "The sensory neurons of touch," *Cell*, vol. 79, no. 4, pp. 618–639, 2014.

[11] H. P. Saal and S. J. Bensmaia, "Touch is a team effort: Interplay of submodalities in cutaneous sensibility," *Trends Neurosci*, vol. 37, no. 12, pp. 689–697, 2014.

[12] E. V. Okorokova, Q. He, and S. J. Bensmaia, "Biomimetic encoding model for restoring touch in bionic hands through a nerve interface," *J. Neural Eng.*, vol. 15, no. 6, 2018, Art. no. 066033.

[13] T. R. Clites *et al.*, "Proprioception from a Neurally-controlled bionic prosthesis," *Sci. Transl. Med.*, vol. 10, no. 443, 2018, Art. no. 443.

[14] S. Gilman, "Joint position sense and vibration sense: Anatomical organisation and assessment," *J. Neurol. Neurosurg. Psychiatry*, vol. 73, no. 5, pp. 473–477, Nov. 2002.

[15] J. C. Tuthill and E. Azim, "Proprioception," *Curr. Biol.*, vol. 28, no. 5, pp. R194–R203, 2018.

[16] B. B. Edin and N. Johansson, "Skin strain patterns provide kinaesthetic information to the human central nervous system," *J. Physiol.*, vol. 487, no. 1, pp. 243–251, Aug. 1995.

[17] E. Raveh, J. Friedman, and S. Portnoy, "Visuomotor behaviors and performance in a dual-task paradigm with and without vibrotactile feedback when using a myoelectric controlled hand," *Assist. Technol.*, vol. 30, no. 5, pp. 274–280, Oct. 2018.

[18] E. D'Anna *et al.*, "A somatotopic bidirectional hand prosthesis with transcutaneous electrical nerve stimulation based sensory feedback," *Sci. Rep.*, vol. 7, no. 1, pp. 1–15, 2017.

[19] J. A. George *et al.*, "Biomimetic sensory feedback through peripheral nerve stimulation improves dexterous use of a bionic hand," *Sci. Robot.*, vol. 4, no. 32, 2019, Art. no. 32.

[20] M. A. Schiefer, E. L. Graczyk, S. M. Sidik, D. W. Tan, and D. J. Tyler, "Artificial tactile and proprioceptive feedback improves performance and confidence on object identification tasks," *PLoS One*, vol. 13, no. 12, Dec. 2018, Art. no. e0207659.

[21] C. Pasluosta, P. Kiele, and T. Stieglitz, "Paradigms for restoration of somatosensory feedback via stimulation of the peripheral nervous system," *Clin. Neurophysiol.*, vol. 129, no. 4, pp. 851–862, 2018.

[22] S. Wendelken *et al.*, "Restoration of motor control and proprioceptive and cutaneous sensation in humans with prior upper-limb amputation via multiple Utah Slanted Electrode Arrays (USEAs) implanted in residual peripheral arm nerves," *J. Neuroeng. Rehabil.*, vol. 14, no. 1, pp. 1–17, 2017.

[23] K. Kim and J. E. Colgate, "Haptic feedback enhances grip force control of sEMG-controlled prosthetic hands in targeted reinnervation amputees," *IEEE Trans. Neural Syst. Rehabil. Eng.*, vol. 20, no. 6, pp. 798–805, Nov. 2012.

[24] J. L. Sullivan *et al.*, "Multi-sensory stimuli improve distinguishability of cutaneous Haptic Cues," *IEEE Trans. Haptics*, vol. 13, no. 2, pp. 286–297, Apr.–Jun. 2020.

[25] A. Ajoudani *et al.*, "Exploring teleimpedance and tactile feedback for intuitive control of the pisa/IIT soft hand," *IEEE Trans. Haptics*, vol. 7, no. 2, pp. 203–215, Apr.–Jun. 2014.

[26] L. Vargas, G. Whitehouse, H. Huang, Y. Zhu, and X. Hu, "Evoked haptic sensation in the hand with concurrent non-invasive nerve stimulation," *IEEE Trans. Biomed. Eng.*, vol. 66, no. 10, pp. 2761–2767, Oct. 2019.

[27] H. Shin, Z. Watkins, H. H. Huang, Y. Zhu, and X. Hu, "Evoked haptic sensations in the hand via non-invasive proximal nerve stimulation," *J. Neural Eng.*, vol. 15, no. 4, Aug. 2018, Art. no. 046005.

[28] T. J. Arakeri, B. A. Hasse, and A. J. Fuglevand, "Object discrimination using electrotactile feedback," *J. Neural Eng.*, vol. 15, no. 4, 2018.

[29] E. D'Anna *et al.*, "A closed-loop hand prosthesis with simultaneous intraneural tactile and position feedback," *Sci. Robot.*, vol. 4, no. 27, Feb. 2019, Art. no. 046007.

[30] H. J. B. Witteveen, H. S. Rietman, and P. H. Veltink, "Vibrotactile grasping force and hand aperture feedback for myoelectric forearm prosthesis users," *Prosthet. Orthot. Int.*, vol. 39, no. 3, pp. 204–212, Jun. 2015, Art. no. eaau8892.

[31] A. R. Krueger, P. Giannoni, V. A. Shah, M. Casadio, and R. Scheidt, "Supplemental vibrotactile feedback control of stabilization and reaching actions of the arm using limb state and position error encodings," *J. Neuroeng. Rehabil.*, vol. 14, no. 1, pp. 1–23, Dec. 2017.

[32] T. Gathmann, S. F. Atashzar, P. G. S. Alva, and D. Farina, "Wearable dual-frequency vibrotactile system for restoring force and stiffness perception," *IEEE Trans. Haptics*, vol. 13, no. 1, pp. 191–196, Jan. 2020.

[33] H. J. B. Witteveen, F. Luft, J. S. Rietman, and P. H. Veltink, "Stiffness feedback for myoelectric forearm prostheses using vibrotactile stimulation," *IEEE Trans. Neural Syst. Rehabil. Eng.*, vol. 22, no. 1, pp. 53–61, 2014.

[34] D. Zhang, H. Xu, P. B. Shull, J. Liu, and X. Zhu, "Somatotopical feedback versus non-somatotopical feedback for phantom digit sensation on amputees using electrotactile stimulation," *J. Neuroeng. Rehabil.*, vol. 12, no. 1, pp. 1–11, 2015.

[35] A. S. Wycherley, P. S. Helliwell, and H. A. Bird, "A novel device for the measurement of proprioception in the hand," *Rheumatology*, vol. 44, no. 5, pp. 638–641, May 2005.

[36] E. Tidoni, G. Fusco, D. Leonardis, A. Frisoli, M. Bergamasco, and S. M. Aglioti, "Illusory movements induced by tendon vibration in right- and left-handed people," *Exp. Brain Res*, vol. 233, no. 2, pp. 375–383, 2015.

[37] B. Stephens-Fripp, G. Alici, and R. Mutlu, "A review of non-invasive sensory feedback methods for transradial prosthetic hands," *IEEE Access*, vol. 6, pp. 6878–6899, 2018, [Online]; Available https://ieeexplore.ieee.org/document/8253455.

[38] R. A. Armstrong, "When to use the Bonferroni correction," *Ophthalmic Physiol. Opt.*, vol. 34, no. 5, pp. 502–508, Sep. 2014.

[39] P. G. Sagastegui Alva, S. Muceli, S. F. Atashzar, L. William, and D. Farina, "Wearable multichannel haptic device for encoding proprioception in the upper limb," *J. Neural Eng.*, vol. 17, no. 5, Oct. 2020, Art. no. 056035.

[40] N. Dunkelberger *et al.*, "Improving perception accuracy with multi-sensory haptic cue delivery," in *Proc. EuroHaptics*, vol. 1, 2018, pp. 289–301.

[41] G. Valle *et al.*, "Hand control with invasive feedback is not impaired by increased cognitive load," *Front. Bioeng. Biotechnol.*, vol. 8, pp. 1–7, Apr. 2020.

[42] J. F. Hahn, "Vibrotactile adaptation and recovery measured by two methods.," *J. Exp. Psychol.*, vol. 71, no. 5, pp. 655–658, 1966.

[43] L. Vargas, H. H. Huang, Y. Zhu, and X. Hu, "Static and dynamic proprioceptive recognition through vibrotactile stimulation," *J. Neural Eng.*, vol. 18, no. 4, Art. no. 046093, Aug. 2021.

[44] S. B. Godfrey *et al.*, "The SoftHand Pro: Functional evaluation of a novel, flexible, and robust myoelectric prosthesis," *PLoS One*, vol. 13, no. 10, Oct. 2018, Art. no. e0205653.

[45] T. B. Scalha, E. Miyasaki, N. M. F. V. Lima, and G. Borges, "Correlations between motor and sensory functions in upper limb chronic hemiparetics after stroke," *Arq. Neuropsiquiatr.*, vol. 69, no. 4, pp. 624–629, Aug. 2011.

[46] S. Hunter and P. Crome, "Hand function and stroke," *Rev. Clin. Gerontol.*, vol. 12, no. 1, pp. 68–81, Feb. 2002.

[47] H. Liu, L. Song, and T. Zhang, "Changes in brain activation in stroke patients after mental practice and physical exercise: A functional MRI study," *Neural Regen. Res.*, vol. 9, no. 15, pp. 1474–1484, 2014.

[48] L. Liu, G. Liu, and Y. Zhang, "More identifiable stiffness feedback for dexterous hand teleoperation in unknown environment," *Proc. Int. Conf. Virtual Real. Vis. ICVRV 2016*, 2016, pp. 312–316.

[49] T. L. Gibo, A. J. Bastian, and A. M. Okamura, "Grip force control during virtual object interaction: Effect of force feedback, accuracy demands, and training," *IEEE Trans. Haptics*, vol. 7, no. 1, pp. 37–47, Jan.–Mar. 2014.

[50] J. D. Brown *et al.*, "Understanding the role of haptic feedback in a teleoperated/prosthetic grasp and lift task," in *Proc. World Haptics Conf.*, 2013, pp. 271–276.

[51] T. R. Makin and S. J. Bensmaia, "Stability of sensory topographies in adult cortex," *Trends Cogn. Sci.*, vol. 21, no. 3, pp. 195–204, Mar. 2017.

[52] J. P. Hunter, "Dissociation of phantom limb phenomena from stump tactile spatial acuity and sensory thresholds," *Brain*, vol. 128, no. 2, pp. 308–320, Dec. 2004.

[53] H. Teuber *et al.*, "Reorganization of sensory function in amputation stumps - 2-point discrimination," *Fed. Proc.*, vol. 8, no. 1, pp. 156–156, 1949.

[54] D. J. O'Boyle, C. E. Moore, E. Poliakoff, R. Butterworth, A. Sutton, and F. W. Cody, "Human locognosic acuity on the arm varies with explicit and implicit manipulations of attention: Implications for interpreting elevated tactile acuity on an amputation stump," *Neurosci. Lett.*, vol. 305, no. 1, pp. 37–40, Jun. 2001.

[55] C. Dai and X. Hu, "Finger joint angle estimation based on motoneuron discharge activities," *IEEE J. Biomed. Heal. Inform.*, vol. 24, no. 3, pp. 760–767, Mar. 2020.

[56] Y. Zheng and X. Hu, "Real-time isometric finger extension force estimation based on motor unit discharge information," *J. Neural Eng.*, vol. 16, no. 6, Oct. 2019, Art. no. 066006.

[57] M. Sartori, G. Durandau, S. Došen, and D. Farina, "Robust simultaneous myoelectric control of multiple degrees of freedom in wrist-hand prostheses by real-time neuromusculoskeletal modeling," *J. Neural Eng.*, vol. 15, no. 6, Dec. 2018, Art. no. 066026.

[58] D. L. Crouch and H. Huang, "Lumped-parameter electromyogram-driven musculoskeletal hand model: A potential platform for real-time prosthesis control," *J. Biomech.*, vol. 49, no. 16, pp. 3901–3907, Dec. 2016.